ASYMPTOTIC HOMOGENIZATION MODEL FOR 3D GRID-REINFORCED COMPOSITE STRUCTURES WITH GENERALLY ORTHOTROPIC REINFORCEMENTS

A.L. Kalamkarov[a*], E.M.Hassan[a], A.V. Georgiades[b], M.A. Savi[c]

[a] Department of Mechanical Engineering, Dalhousie University, Halifax, Nova Scotia, B3J 2X4, Canada

[b] Department of Mechanical Engineering and Materials Science and Engineering, Cyprus University of Technology, Limassol, Cyprus

[c] Department of Mechanical Engineering, COPPE, Universidade Federal do Rio de Janeiro, Rio de Janeiro, RJ, Brazil

Abstract

The asymptotic homogenization method is used to develop a comprehensive micromechanical model pertaining to three-dimensional composite structures with an embedded periodic grid of generally orthotropic reinforcements. The model developed transforms the original boundary-value problem into a simpler one characterized by some effective elastic coefficients. These effective coefficients are shown to depend only on the geometric and material parameters of the unit cell and are free from the periodicity complications that characterize their original material counterparts. As a consequence they can be used to study a wide variety of boundary value problems associated with the composite of a given microstructure. The developed model is applied to different examples of orthotropic composite structures with cubic, conical and diagonal reinforcement orientations. It is shown in these examples that the model allows for

[*] Corresponding Author Tel.: +1-902-494-6072;
E-mail address: alex.kalamkarov@dal.ca (A.L.Kalamkarov)

complete flexibility in designing a grid-reinforced composite structure with desirable elastic coefficients to conform to any engineering application by changing some material and/or geometric parameter of interest. It is also shown in this work that in the limiting particular case of 2D grid-reinforced structure with isotropic reinforcements our results converge to the earlier published results.

Keywords: Asymptotic Homogenization; Grid-Reinforced Composite Structures; Orthotropic reinforcement; Effective Elastic Coefficients.

1. Introduction

Recent years have witnessed a considerable increase in the use composite materials in various engineering applications such as aerospace, automotive, and marine engineering, medical prosthetic devices, sports infrastructure, and recreational goods. Large-scale introduction and continued use of composite materials into novel applications can be significantly facilitated if their macroscopic behavior can be predicted at the design stage. Accordingly, comprehensive micromechanical models must be developed. To obtain more effective micromechanical models which can accurately predict the mechanical properties of composite materials, it is common practice to analyze composite materials using two scales. These two scales are often referred to as microscopic and macroscopic levels of analysis. In the microscopic level, one attempts to recognize the fine details of the composite material structure, i.e., the behavior and individual characteristics of the various constituents such as the reinforcing elements (e.g., long fibers, particles, whiskers) and matrix material, while the macroscopic level amounts to dealing with the global behavior of composite material structure as an individual entity. Effective formulation of the pertinent micromechanical model must take into consideration both

the local and the global aspects of the composite. Therefore, to realistically reflect the properties and characteristics of the composite structure, the micromechanical model developed should be rigorous enough to enable the consideration of the spatial distribution, characteristics, mechanical properties, and behavior of different constituents at the local level, but, at the same time, not too complicated to be used via straight-forward analytic and numerical treatments.

Modeling of composites made up of inclusions embedded in a matrix has been a subject of interest of many researchers in the past half-century. Noteworthy among the earlier models are the works of Eshelby (1957) [1], Hashin (1962) [2], Hill (1963, 1965) [3] and [4], Hashin & Shtrikman (1963a, 1963b) [5] and [6], Hashin & Rosen (1964) [7]. Hashin & Shtrikman (1963a, 1963b) [5] and [6] used variational principles to obtain upper and lower bounds for the effective elastic moduli (1963a) [5] as well as the effective electrical and thermal conductivities (1963b) [6] of multiphase composites with quasi-isotropic global characteristics. Later on, Milton (1981, 1982) [8] and [9] obtained higher-order bounds for the elastic, electromagnetic, and transport properties of two-component macroscopically homogenous and isotropic composites given the properties of the individual constituents. More recently, Drugan & Willis (1996) [10] and Drugan (2003) [11], employed the Hashin-Shtrikman variational principles to analyze two-phase composites with random microstructure. A numerical implementation of this work was carried out by Segurado & Llorca (2002) [12].

Other significant early results can be found in the work of Budiansky (1965) [13], Russel (1973) [14]. Mori & Tanaka (1973) [15] in their micromechanical approach obtained closed-form expressions for the elastic properties of two-phase composites. This

model is accurate for microscale particles. For the case of nanoscale inclusions however, it has been shown that there exists an interphase region between the inclusion and the matrix (i.e. there are no longer only two distinct phases in the composite - a key assumption in the Mori and Tanaka model), and the length scale of this interphase region is of the same order of magnitude as the inclusions themselves. Thus the Mori and Tanaka model is not valid and alternative approaches must be used, see for example Odegard et al (2003) [16], Sevostianov & Kachanov (2006) [17].

Other related work can be found in Walpole (1966, 1969) [18] and [19], Halpin (1969) [20], Sendeckyj (1974) [21], Hashin (1983) [22], Torquato & Stell (1985) [23], Vinson & Sierokowski (1986) [24], Milton & Kohn (1988) [25], Teply & Dvorak (1988) [26], Vieira Carneiro & Savi (2000) [27], and more recently in Christensen (1990) [28], Torquato (1991), Vasiliev (1993) [29], Kalamkarov & Liu (1998) [30], Zeman & Šejnoha (2001) [31], Haj-Ali & Kilic (2003) [32], Luccioni (2006) [33].

Partial differential equations describing the behavior of composite materials with multiple regularly spaced inclusions are characterized by the presence of rapidly varying coefficients due to the presence of numerous periodically (or nearly periodically) embedded inclusions in close proximity to one another. To treat these equations analytically, one, therefore, has to consider two sets of spatial variables, one for the microscopic characteristics of the constituents and the other for the macroscopic behavior of the composite under investigation. The presence of the microscopic and macroscopic scales in the original problem frequently renders the pertinent partial differential equations extremely difficult to solve. Clearly, the ensuing analysis would be significantly simplified if the two scales could be decoupled and each one handled

separately; one technique that permits us to accomplish precisely this is the asymptotic homogenization method. The mathematical framework of asymptotic homogenization can be found in Bensoussan et al. (1978) [34], Sanchez-Palencia (1980) [35], Bakhvalov & Panasenko (1984) [36]. In recent years, asymptotic homogenization method has been used to analyze periodic composite and smart structures, see e.g. the pioneering work by Duvaut (1976) [37] on inhomogeneous plates. Other work can be found in Caillerie (1984) [38] in his heat conduction studies pertaining to thin elastic and periodic plates, Kohn & Vogelius (1984, 1985) [39] and [40] who used asymptotic homogenization to analyze the pure bending of a linearly elastic homogeneous plate with rapidly varying thickness, and Kalamkarov (1992) [41] who examined a wide variety of elasticity and thermoelasticity problems pertaining to composite materials and thin-walled composite structures, reinforced plates and shells. Kalamkarov & Kolpakov (2001) [42] dealt with the piezoelastic problem for a three-dimensional thin composite solid and calculated the effective elastic and piezoelectric coefficients of the homogenized structure. Kalamkarov & Georgiades (2002a, 2002b) [43] and [44] derived expressions for the effective elastic, piezoelectric, and hygrothermal expansion coefficients for general three-dimensional periodic smart composite structures. The boundary-layer type asymptotic expansions are developed in [44] to satisfy the boundary conditions in the homogenization model. Kalamkarov & Georgiades, 2004 [45] and Georgiades & Kalamkarov, 2004, [46] developed comprehensive asymptotic homogenization models for smart composite plates with rapidly varying thickness and periodically arranged actuators. These models were subsequently used to determine general expressions for the effective coefficients of the homogenized plates and the work was illustrated by means of different examples such as

constant-thickness laminates and wafer- and rib-reinforced smart composite plates; Georgiades et al. (2006) [47] applied a general three-dimensional micromechanical model pertaining to thin smart composite plates reinforced with a network of cylindrical reinforcements that may also exhibit piezoelectric behavior. Challagulla et al. (2007) [48] developed a comprehensive three-dimensional asymptotic homogenization model pertaining to globally anisotropic periodic composite structures reinforced with a spatial network of isotropic reinforcements. Other work can be found in Andrianov et al (1985) [49], Challagulla et al. (2008) [50], Guedes & Kikuchi (1990) [51], Andrianov et al. (2006) [52], Kalamkarov et al (2006) [53], Saha et al (2007a, 2007b) [54] and [55].

The present paper proposes a novel asymptotic homogenization model for three-dimensional grid-reinforced periodic composite structures, see Fig. 1. Most importantly. in this work we consider the reinforcements made of generally orthotropic material which renders the pertinent analysis significantly more complicated than in simpler case of isotropic reinforcements.

Following this introduction the rest of the paper is organized as follows: The basic problem formulation and model development are presented in Section 2. Section 3 derives the general model for three-dimensional grid-reinforced composite structures and Sections 4 and 5 apply it to analyze and discuss various examples of a particular importance. Finally, Section 6 concludes the paper.

2. Asymptotic Homogenization Model for Three-Dimensional Structures

2.1 General Model

Consider a general composite structure representing an inhomogeneous solid occupying domain Ω with boundary $\partial\Omega$ that contains a large number of periodically

arranged reinforcements as shown in Fig. 2(a). It can be observed that this periodic structure is obtained by repeating a small unit cell Y in the domain Ω, see Fig. 2(b).

The elastic deformation of this structure can be described by means of the following boundary-value problem:

$$\frac{\partial \sigma_{ij}^{\varepsilon}}{\partial x_j} = f_i \ \text{ in } \ \Omega\,, \ \ u_i^{\varepsilon}(\mathbf{x}) = 0 \ \text{ on } \partial\Omega \tag{1}$$

$$\sigma_{ij}^{\varepsilon}\left(\mathbf{x}, \frac{\mathbf{x}}{\varepsilon}\right) = C_{ijkl}\left(\frac{\mathbf{x}}{\varepsilon}\right) e_{kl}^{\varepsilon}\left(\mathbf{x}, \frac{\mathbf{x}}{\varepsilon}\right) \tag{2}$$

$$e_{ij}^{\varepsilon}\left(\mathbf{x}, \frac{\mathbf{x}}{\varepsilon}\right) = \frac{1}{2}\left[\frac{\partial u_i}{\partial x_j}\left(\mathbf{x}, \frac{\mathbf{x}}{\varepsilon}\right) + \frac{\partial u_j}{\partial x_i}\left(\mathbf{x}, \frac{\mathbf{x}}{\varepsilon}\right)\right] \tag{3}$$

Here and in the sequel, all indexes assume values of 1,2,3, and the summation convention is adopted, C_{ijkl} is the tensor of elastic coefficients, e_{kl} is the strain tensor which is a function of the displacement field u_i, and, finally, f_i represent body forces. It is assumed in Eq. (2) that the C_{ijkl} coefficients are all periodic with a unit cell Y of characteristic dimension ε. Small parameter ε is made non-dimensional by dividing the characteristic size of the unit cell by a certain characteristic dimension of the overall structure. Consequently, the periodic composite structure in Fig. 2 is seen to be made up of a large number of unit cells periodically arranged within the domain Ω.

2.2 Asymptotic Expansions, Governing Equations and Unit Cell Problems

The development of asymptotic homogenization model for the three-dimensional smart composite structures can be found in Kalamkarov & Georgiades (2002a&b) [43] and [44]. In this Section, only a brief overview of the steps involved in the development

of the model are given in so far as it represents the starting point of our current work. The first step is to define the so-called "fast" or microscopic variables according to:

$$y_i = \frac{x_i}{\varepsilon},\ i = 1, 2, 3 \tag{4a}$$

As a consequence of introducing the fast variable ***y*** the derivatives must be transformed according to:

$$\frac{\partial}{\partial x_i} \to \frac{\partial}{\partial x_i} + \frac{1}{\varepsilon}\frac{\partial}{\partial y_i} \tag{4b}$$

The boundary value problem and corresponding stress field defined in Eqs. (1) and (2) are thus readily transformed into the following expressions:

$$\frac{\partial \sigma_{ij}^{\varepsilon}}{\partial x_j} + \frac{1}{\varepsilon}\frac{\partial \sigma_{ij}^{\varepsilon}}{\partial y_j} = f_i \quad \text{in } \Omega, \quad u_i^{\varepsilon} = 0 \text{ on } \partial\Omega \tag{5}$$

$$\sigma_{ij}^{\varepsilon}(\mathbf{x},\mathbf{y}) = C_{ijkl}(\mathbf{y})\frac{\partial u_k}{\partial x_l}(\mathbf{x},\mathbf{y}) \tag{6}$$

The next step is to consider the following asymptotic expansions in terms of the small parameter ε:

(i) Asymptotic expansion for the displacement field:

$$\mathbf{u}^{\varepsilon}(\mathbf{x},\mathbf{y}) = \mathbf{u}^{(0)}(\mathbf{x},\mathbf{y}) + \varepsilon\mathbf{u}^{(1)}(\mathbf{x},\mathbf{y}) + \varepsilon^2\mathbf{u}^{(2)}(\mathbf{x},\mathbf{y}) + \ldots \tag{7}$$

(ii) Asymptotic expansion for the stress field:

$$\sigma_{ij}^{\varepsilon}(\mathbf{x},\mathbf{y}) = \sigma_{ij}^{(0)}(\mathbf{x},\mathbf{y}) + \varepsilon\sigma_{ij}^{(1)}(\mathbf{x},\mathbf{y}) + \varepsilon^2\sigma_{ij}^{(2)}(\mathbf{x},\mathbf{y}) + \ldots \tag{8}$$

It is understood that all functions in ***y*** are collectively periodic with the unit cell Y as shown in 2(b). By substituting Eqs. (4a)–(4b) and (6) into Eq. (5) and considering at the same time the periodicity of $\mathbf{u}^{(i)}$ in ***y*** one can readily eliminate the microscopic variable ***y*** from the first term $\mathbf{u}^{(0)}$ in the asymptotic displacement field expansion to show that it depends only on the macroscopic variable ***x***. Subsequently, by substituting Eq. (8) into

Eq. (5) and considering terms with like powers of ε one obtains a series of differential equations the first two expressions of which are:

$$\frac{\partial \sigma_{ij}^{(0)}}{\partial y_j} = 0 \tag{9a}$$

$$\frac{\partial \sigma_{ij}^{(1)}}{\partial y_j} + \frac{\partial \sigma_{ij}^{(0)}}{\partial x_j} = f_i \tag{9b}$$

where,

$$\sigma_{ij}^{(0)} = C_{ijkl}\left(\frac{\partial u_k^{(0)}}{\partial x_l} + \frac{\partial u_k^{(1)}}{\partial y_l} \right) \tag{10a}$$

$$\sigma_{ij}^{(1)} = C_{ijkl}\left(\frac{\partial u_k^{(1)}}{\partial x_l} + \frac{\partial u_k^{(2)}}{\partial y_l} \right) \tag{10b}$$

Combination of Eqs. (9a) and (10a) leads to the following expression:

$$\frac{\partial}{\partial y_j}\left(C_{ijkl} \frac{\partial u_k^{(1)}(\mathbf{x},\mathbf{y})}{\partial y_l} \right) = -\frac{\partial C_{ijkl}(\mathbf{y})}{\partial y_j} \frac{\partial u_k^{(0)}(\mathbf{x})}{\partial x_l} \tag{11}$$

The separation of variables on the right-hand-side of Eq. (11) prompts us to write down the solution for $\mathbf{u}^{(1)}$ as:

$$u_m^{(1)}(\mathbf{x},\mathbf{y}) = V_m(\mathbf{x}) + \frac{\partial u_k^{(0)}(\mathbf{x})}{\partial x_l} N_m^{kl}(\mathbf{y}) \tag{12}$$

where functions N_m^{kl} are periodic in $\boldsymbol{y}$ and satisfy

$$\frac{\partial}{\partial y_j}\left(C_{ijmn}(\mathbf{y}) \frac{\partial N_m^{kl}(\mathbf{y})}{\partial y_n} \right) = -\frac{\partial C_{ijkl}}{\partial y_j} \tag{13}$$

while the function $V_m(x)$ is the homogenous solution of Eq. (12) and satisfies

$$\frac{\partial}{\partial y_j}\left(C_{ijmn}(\mathbf{y}) \frac{\partial V_m(\mathbf{y})}{\partial y_n} \right) = 0 \tag{14}$$

One observes that Eq. (13) depends entirely on the fast variable $\boldsymbol{y}$ and is thus solved on the domain Y of the unit cell, remembering at the same time that both C_{ijkl} and N_m^{kl} are Y-periodic in $\boldsymbol{y}$ .Consequently, Eq. (13) is appropriately referred to as the *unit-cell problem.*

The next important step in the model development is the homogenization procedure. This is carried out by first substituting Eq. (12) into Eq. (10a), and combining the result with Eq. (9b). The resulting expression is eventually integrated over the domain Y of the unit cell (with volume $|\mathrm{Y}|$) remembering to treat x_i as a parameter as far as integration with respect to y_j is concerned. This yields:

$$\frac{1}{|\mathrm{Y}|}\int_{\mathrm{Y}}\frac{\partial\sigma_{\mathrm{ij}}^{(1)}(\mathbf{x},\mathbf{y})}{\partial \mathrm{y}_{\mathrm{j}}}\mathrm{dv}+\tilde{\mathrm{C}}_{\mathrm{ijkl}}\frac{\partial^2 \mathrm{u}_{\mathrm{k}}^{(0)}(\mathbf{x})}{\partial \mathrm{x}_{\mathrm{j}}\partial \mathrm{x}_{\mathrm{l}}}=\mathrm{f}_{\mathrm{i}} \tag{15}$$

where the following definition is introduced:

$$\tilde{\mathrm{C}}_{\mathrm{ijkl}}=\frac{1}{|\mathrm{Y}|}\int_{\mathrm{Y}}\left(\mathrm{C}_{\mathrm{ijkl}}(\mathbf{y})+\mathrm{C}_{\mathrm{ijmn}}(\mathbf{y})\frac{\partial \mathrm{N}_{\mathrm{m}}^{\mathrm{kl}}}{\partial \mathrm{y}_{\mathrm{n}}}\right)\mathrm{dv} \tag{16}$$

The coefficients $\tilde{C}_{ijkl}$ denote the homogenized or effective elastic coefficients. It is noticed that the effective elastic coefficients are free from the inhomogeneity complications that characterize their actual rapidly varying material counterparts, C_{ijkl}, and as such, are more amenable to analytical and numerical treatment. The effective coefficients shown above are universal in nature and can be used to study a wide variety of boundary value problems associated with a given composite structure.

3. Three-Dimensional Grid-Reinforced Composite Structures

In the subsequent Sections we will be concerned with the problem of a general macroscopically anisotropic 3D composite structure reinforced with N families of reinforcements, see for instance Fig. 1 where an explicit case of 3 families of

reinforcements is shown. We assume the members of each family are made of dissimilar, generally orthotropic materials and have relative orientation angles $\theta_1^n, \theta_2^n, \theta_3^n$ (where n = 1, 2, …., *N*) with the y_1, y_2, y_3 axes respectively. It is further assumed that the orthotropic reinforcements have significantly higher elasticity moduli than the matrix material, so we are justified in neglecting the contribution of the matrix phase in the analytical treatment. Clearly, for the particular case of framework or lattice network structures the surrounding matrix is absent and this is modeled by assuming zero matrix rigidity. The nature of the network structure of Fig. 1 is such that it would be more efficient if we first considered a simpler type of unit cell made of only a single reinforcement as shown in Fig. 3. Having solved this, the effective elastic coefficients of more general structures with several families of reinforcements can readily be determined by the superposition of the solution for each of them found separately. In following this procedure, one must naturally accept the error incurred at the regions of intersection between the reinforcements. However, our approximation will be quite accurate because these regions of intersection are highly localized and do not contribute significantly to the integral over the entire unit cell domain. A complete mathematical justification for this argument in the form of the so-called principle of the split homogenized operator has been provided by Bakhvalov and Panasenko (1984) [36]. In order to calculate the effective coefficients for the simpler structure of Fig. 3, unit cell problem given by Eq. (13) must be solved and, subsequently, Eq. (16) must be applied.

3.1 Problem Formulation

The problem formulation for the structure shown in Fig. 3 begins with the introduction of the following notation:

$$b_{ij}^{kl} = C_{ijmn}(\mathbf{y})\frac{\partial N_m^{kl}(\mathbf{y})}{\partial y_n} + C_{ijkl} \tag{17}$$

With this definition in mind the unit cell of the problem given by Eq. (13) becomes:

$$\frac{\partial}{\partial y_j} b_{ij}^{kl} = 0 \tag{18}$$

We assume perfect bonding conditions at the interface between the reinforcements and the matrix. This assumption translates into the following interface conditions:

$$N_n^{kl}(r)\big|_s = N_n^{kl}(m)\big|_s \tag{19}$$

$$b_{ij}^{kl}(r)n_j\big|_s = b_{ij}^{kl}(m)n_j\big|_s \tag{20}$$

In Eqs. (19) and (20) the suffixes *"r", "m",* and *"s"* denote the "reinforcement", "matrix", and reinforcement/matrix interface, respectively; while n_j denote the components of the unit normal vector at the interface. As noted earlier, we will further assume that $C_{ijmn}(m) = 0,$ and hence $b_{ij}^{kl}(m) = 0$. Therefore, the interface condition (20) becomes:

$$b_{ij}^{kl}(r)n_j\big|_s = 0 \tag{21}$$

To summarize, the final unit cell problem that must be solved in conjunction with Eq. (19) for the three-dimensional grid structure reinforced with a single family of orthotropic reinforcements is:

$$\frac{\partial}{\partial y_j} b_{ij}^{kl} = 0 \tag{22}$$

$$b_{ij}^{kl}(r)n_j\big|_s = 0 \tag{23}$$

3.2 Coordinate Transformation

Before solving the unit cell problem given by Eqs. (22) and (23) we will perform a coordinate transformation of the microscopic coordinate system $\{y_1, y_2, y_3\}$ onto the new

coordinate system $\{\eta_1, \eta_2, \eta_3\}$, as shown in Fig.4. This transformation is defined by having the η_1 coordinate axis coincide with the longitudinal direction of the reinforcement and the other two axes, η_2 and η_3 perpendicular to it.

Thus, derivatives transform according to:

$$\frac{\partial}{\partial y_j} = q_{ij} \frac{\partial}{\partial \eta_i} \tag{24}$$

where q_{ij} are the components of the direction cosines characterizing the axes rotation.

Based on the selection of the above coordinate system, we note that since the reinforcement is oriented along the η_1 coordinate axis, the problem at hand becomes independent of η_1 and will only depend on η_2 and η_3. As a result, the overall solution order is reduced by one and the ensuing analysis is simplified.

3.3 Method for Determining Elastic Coefficients

With reference to Fig. 4, we begin by rewriting Eqs. (22) and (23) in terms of the η_i coordinates to get:

$$b_{ij}^{kl} = C_{ijkl}(\mathbf{y}) + C_{ijmn} q_{pn} \frac{\partial N_m^{kl}(\mathbf{y})}{\partial \eta_p} \tag{25a}$$

$$\left(b_{ij}^{kl} q_{2j} n_2'(r) + b_{ij}^{kl} q_{3j} n_3'(r) \right)\Big|_s = 0 \tag{25b}$$

Here, n_2' and n_3' are the components of the unit normal vector in the new coordinate system. Expanding Eq. (25a) and keeping in mind the independency of the unit cell problem on η_1 yields:

$$\begin{aligned} b_{ij}^{kl} = C_{ijkl} &+ C_{ijm1} q_{21} \frac{\partial N_m^{kl}}{\partial \eta_2} + C_{ijm2} q_{22} \frac{\partial N_m^{kl}}{\partial \eta_2} + C_{ijm3} q_{23} \frac{\partial N_m^{kl}}{\partial \eta_2} + \\ & C_{ijm1} q_{31} \frac{\partial N_m^{kl}}{\partial \eta_3} + C_{ijm2} q_{32} \frac{\partial N_m^{kl}}{\partial \eta_3} + C_{ijm3} q_{33} \frac{\partial N_m^{kl}}{\partial \eta_3} \end{aligned} \tag{26}$$

Apparently, Eqs. (25a), (25b) can be solved by assuming a linear variation of the local functions N_m^{kl} with respect to η_2 and η_3, i.e.

$$\begin{aligned} N_1^{kl} &= \lambda_1^{kl}\eta_2 + \lambda_2^{kl}\eta_3 \\ N_2^{kl} &= \lambda_3^{kl}\eta_2 + \lambda_4^{kl}\eta_3 \\ N_3^{kl} &= \lambda_5^{kl}\eta_2 + \lambda_6^{kl}\eta_3 \end{aligned} \tag{27}$$

where λ_i^{kl} are constants to be determined from the boundary conditions. The functions b_{ij}^{kl} can be written from Eqs. (26) and (27) as follows:

$$\begin{aligned}
b_{11}^{kl} &= C_{11kl} + \begin{bmatrix} \lambda_1^{kl}\{C_{11}q_{21} + C_{16}q_{22} + C_{15}q_{23}\} + \lambda_2^{kl}\{C_{11}q_{31} + C_{16}q_{32} + C_{15}q_{33}\} + \\ +\lambda_3^{kl}\{C_{16}q_{21} + C_{12}q_{22} + C_{14}q_{23}\} + \lambda_4^{kl}\{C_{16}q_{31} + C_{12}q_{32} + C_{14}q_{33}\} + \\ +\lambda_5^{kl}\{C_{15}q_{21} + C_{14}q_{22} + C_{13}q_{23}\} + \lambda_6^{kl}\{C_{15}q_{31} + C_{14}q_{32} + C_{13}q_{33}\} \end{bmatrix} \\
b_{22}^{kl} &= C_{22kl} + \begin{bmatrix} \lambda_1^{kl}\{C_{21}q_{21} + C_{26}q_{22} + C_{25}q_{23}\} + \lambda_2^{kl}\{C_{21}q_{31} + C_{26}q_{32} + C_{25}q_{33}\} + \\ +\lambda_3^{kl}\{C_{26}q_{21} + C_{22}q_{22} + C_{24}q_{23}\} + \lambda_4^{kl}\{C_{26}q_{31} + C_{22}q_{32} + C_{24}q_{33}\} + \\ +\lambda_5^{kl}\{C_{25}q_{21} + C_{24}q_{22} + C_{23}q_{23}\} + \lambda_6^{kl}\{C_{25}q_{31} + C_{24}q_{32} + C_{23}q_{33}\} \end{bmatrix} \\
b_{33}^{kl} &= C_{33kl} + \begin{bmatrix} \lambda_1^{kl}\{C_{31}q_{21} + C_{36}q_{22} + C_{35}q_{23}\} + \lambda_2^{kl}\{C_{31}q_{31} + C_{36}q_{32} + C_{35}q_{33}\} + \\ +\lambda_3^{kl}\{C_{36}q_{21} + C_{32}q_{22} + C_{34}q_{23}\} + \lambda_4^{kl}\{C_{36}q_{31} + C_{32}q_{32} + C_{34}q_{33}\} + \\ +\lambda_5^{kl}\{C_{35}q_{21} + C_{34}q_{22} + C_{33}q_{23}\} + \lambda_6^{kl}\{C_{35}q_{31} + C_{34}q_{32} + C_{33}q_{33}\} \end{bmatrix} \\
b_{23}^{kl} &= C_{23kl} + \begin{bmatrix} \lambda_1^{kl}\{C_{41}q_{21} + C_{46}q_{22} + C_{45}q_{23}\} + \lambda_2^{kl}\{C_{41}q_{31} + C_{46}q_{32} + C_{45}q_{33}\} + \\ +\lambda_3^{kl}\{C_{46}q_{21} + C_{42}q_{22} + C_{44}q_{23}\} + \lambda_4^{kl}\{C_{46}q_{31} + C_{42}q_{32} + C_{44}q_{33}\} + \\ +\lambda_5^{kl}\{C_{45}q_{21} + C_{44}q_{22} + C_{43}q_{23}\} + \lambda_6^{kl}\{C_{45}q_{31} + C_{44}q_{32} + C_{43}q_{33}\} \end{bmatrix} \\
b_{13}^{kl} &= C_{13kl} + \begin{bmatrix} \lambda_1^{kl}\{C_{51}q_{21} + C_{56}q_{22} + C_{55}q_{23}\} + \lambda_2^{kl}\{C_{51}q_{31} + C_{56}q_{32} + C_{55}q_{33}\} + \\ +\lambda_3^{kl}\{C_{56}q_{21} + C_{52}q_{22} + C_{54}q_{23}\} + \lambda_4^{kl}\{C_{56}q_{31} + C_{52}q_{32} + C_{54}q_{33}\} + \\ +\lambda_5^{kl}\{C_{55}q_{21} + C_{54}q_{22} + C_{53}q_{23}\} + \lambda_6^{kl}\{C_{55}q_{31} + C_{54}q_{32} + C_{53}q_{33}\} \end{bmatrix} \\
b_{12}^{kl} &= C_{12kl} + \begin{bmatrix} \lambda_1^{kl}\{C_{61}q_{21} + C_{66}q_{22} + C_{65}q_{23}\} + \lambda_2^{kl}\{C_{61}q_{31} + C_{66}q_{32} + C_{65}q_{33}\} + \\ +\lambda_3^{kl}\{C_{66}q_{21} + C_{62}q_{22} + C_{64}q_{23}\} + \lambda_4^{kl}\{C_{66}q_{31} + C_{62}q_{32} + C_{64}q_{33}\} + \\ +\lambda_5^{kl}\{C_{65}q_{21} + C_{64}q_{22} + C_{63}q_{23}\} + \lambda_6^{kl}\{C_{65}q_{31} + C_{64}q_{32} + C_{63}q_{33}\} \end{bmatrix}
\end{aligned} \tag{28}$$

Here C_{IJ} (I, J = 1,2,3, .., 6) are the elastic coefficients of the orthotropic reinforcements in the contracted notation, see ,e.g., Reddy (1997) [56]. These components are obtained from C_{ijkl} by the following replacement of subscripts:

$11 \to 1 \qquad 22 \to 2 \qquad 33 \to 3 \qquad 23 \to 4 \qquad 13 \to 5 \qquad 12 \to 6$

The resulting C_{IJ} are symmetric, $C_{IJ} = C_{JI}$.

It is important to reiterate here that the elastic coefficients in Eq. (28) are referenced with respect to the $\{y_1, y_2, y_3\}$ coordinate system. The relationship between these elastic coefficients and the elastic coefficients associated with the principal material coordinate system of the reinforcing bar, $C^{(p)}_{mnpq}$, is expressed by means of the familiar 4th-order tensor transformation Eq. (29).

$$C_{ijkl} = q_{ir} q_{js} q_{kv} q_{lw} C^{(P)}_{rsvw} \tag{29}$$

Expansion of the interface condition in Eq. (25b) over the subscript j yields:

$$\left((b^{kl}_{i1} q_{21} + b^{kl}_{i2} q_{22} + b^{kl}_{i3} q_{23}) n'_2 + (b^{kl}_{i1} q_{31} + b^{kl}_{i2} q_{32} + b^{kl}_{i3} q_{33}) n'_3 \right)\Big|_s = 0 \tag{30}$$

Substitution of the expressions given in Eq. (28) into Eq. (30) results in the following 6 linear algebraic equations for λ^{kl}_i:

$$\begin{aligned}
&A_1\lambda^{kl}_1 + A_2\lambda^{kl}_2 + A_3\lambda^{kl}_3 + A_4\lambda^{kl}_4 + A_5\lambda^{kl}_5 + A_6\lambda^{kl}_6 + A^{kl}_7 = 0 \\
&A_8\lambda^{kl}_1 + A_9\lambda^{kl}_2 + A_{10}\lambda^{kl}_3 + A_{11}\lambda^{kl}_4 + A_{12}\lambda^{kl}_5 + A_{13}\lambda^{kl}_6 + A^{kl}_{14} = 0 \\
&A_{15}\lambda^{kl}_1 + A_{16}\lambda^{kl}_2 + A_{17}\lambda^{kl}_3 + A_{18}\lambda^{kl}_4 + A_{19}\lambda^{kl}_5 + A_{20}\lambda^{kl}_6 + A^{kl}_{21} = 0 \\
&A_{22}\lambda^{kl}_1 + A_{23}\lambda^{kl}_2 + A_{24}\lambda^{kl}_3 + A_{25}\lambda^{kl}_4 + A_{26}\lambda^{kl}_5 + A_{27}\lambda^{kl}_6 + A^{kl}_{28} = 0 \\
&A_{29}\lambda^{kl}_1 + A_{30}\lambda^{kl}_2 + A_{31}\lambda^{kl}_3 + A_{32}\lambda^{kl}_4 + A_{33}\lambda^{kl}_5 + A_{34}\lambda^{kl}_6 + A^{kl}_{35} = 0 \\
&A_{36}\lambda^{kl}_1 + A_{37}\lambda^{kl}_2 + A_{38}\lambda^{kl}_3 + A_{39}\lambda^{kl}_4 + A_{40}\lambda^{kl}_5 + A_{41}\lambda^{kl}_6 + A^{kl}_{42} = 0
\end{aligned} \tag{31}$$

where A^{kl}_i are constants which depend on the geometric parameters of the unit cell and the material properties of the reinforcement. The explicit expressions for these constants are given in Appendix A. Once the system of Eq. (31) is solved, the determined

λ_i^{kl} coefficients are substituted back into Eq. (28) to obtain the b_{ij}^{kl} coefficients. In turn, these are used to calculate the effective elastic coefficients of the structure of Fig. 3 by integrating over the volume of the unit cell as it will be explained below in Section 3.4. Before closing this Section, it would not be amiss to mention that if we assumed in Eq. (27) polynomials of a higher order, then after following the aforementioned procedure and comparing terms of equal powers of η_2 and η_3, all of the terms would vanish except the linear ones.

3.4 Effective Elastic Coefficients

The effective elastic moduli of the 3D grid-reinforced composite with generally orthotropic reinforcements shown in Fig. 3 are obtained on the basis of integration (16), which, on account of notation (17) becomes:

$$\tilde{C}_{ijkl} = \frac{1}{|Y|}\int_Y b_{ij}^{kl}\,dv \tag{32}$$

Noting that b_{ij}^{kl} are constants, and denoting the length and cross-sectional area of the reinforcement (in coordinates y_1, y_2, y_3) by L and A respectively, and the volume of the unit cell by V, the effective elastic coefiicients become

$$\tilde{C}_{ijkl} = \frac{AL}{V} b_{ij}^{kl} = V_f\, b_{ij}^{kl} \tag{33a}$$

where V_f is the volume fraction of the reinforcement within the unit cell. It can be proved in general that the effective elastic coefficients $\tilde{C}_{ijkl}$ maintain the same symmetry and convexity properites as their actual material counterparts C_{ijkl}, see, e.g., Bakhvalov & Panasenko (1984) [36].

The above derived effective moduli pertain to grid-reinforced structures with a single family of reinforcements. For structures with more than one family of reinforcements the effective moduli can be obtained by superimposition. For instance, the effective elastic coefficients of a grid-reinforced structure with *N* families of generally orthotropic reinforcements will be given by:

$$\tilde{C}_{ijkl} = \sum_{n=1}^{N} V_f^{(n)} b_{ij}^{(n)kl} \tag{33b}$$

where the superscript *(n)* represents the *n-th* reinforcement family.

4. Examples of Grid-Reinforced Structures

The developed micromechanical model and methodology presented in this work are now used to study four different practically important examples of grid-reinforced composite structures with orthotropic reinforcements.

4.1 Example 1 - 3D Cubic Grid-Reinforced Composite with Orthotropic Reinforcement

The first example pertains to the cubic grid-reinforced structure shown in Fig. 1. This structure has three families of generally orthotropic reinforcements, each family oriented along one of the coordinate axes, as shown in Fig. 5.

Noting that in this case $q_{ij} = \delta_{ij}$, where δ_{ij} is the Kronecker Delta, the values of λ_i^{kl} for the reinforcement in the y_1 direction are obtained from Eq. (31) and then substituted into Eq. (28) to determine functions b_{ij}^{kl}.

$$
\begin{aligned}
b_{11}^{kl} &= C_{11kl} + \left[\lambda_1^{kl} C_{16} + \lambda_2^{kl} C_{15} + \lambda_3^{kl} C_{12} + \lambda_4^{kl} C_{14} + \lambda_5^{kl} C_{14} + \lambda_6^{kl} C_{13}\right] \\
b_{22}^{kl} &= C_{22kl} + \left[\lambda_1^{kl} C_{26} + \lambda_2^{kl} C_{25} + \lambda_3^{kl} C_{22} + \lambda_4^{kl} C_{24} + \lambda_5^{kl} C_{24} + \lambda_6^{kl} C_{23}\right] \\
b_{33}^{kl} &= C_{33kl} + \left[\lambda_1^{kl} C_{36} + \lambda_2^{kl} C_{35} + \lambda_3^{kl} C_{32} + \lambda_4^{kl} C_{34} + \lambda_5^{kl} C_{34} + \lambda_6^{kl} C_{33}\right] \\
b_{23}^{kl} &= C_{23kl} + \left[\lambda_1^{kl} C_{46} + \lambda_2^{kl} C_{45} + \lambda_3^{kl} C_{42} + \lambda_4^{kl} C_{44} + \lambda_5^{kl} C_{44} + \lambda_6^{kl} C_{43}\right] \\
b_{13}^{kl} &= C_{13kl} + \left[\lambda_1^{kl} C_{56} + \lambda_2^{kl} C_{55} + \lambda_3^{kl} C_{52} + \lambda_4^{kl} C_{54} + \lambda_5^{kl} C_{54} + \lambda_6^{kl} C_{53}\right] \\
b_{12}^{kl} &= C_{12kl} + \left[\lambda_1^{kl} C_{66} + \lambda_2^{kl} C_{65} + \lambda_3^{kl} C_{62} + \lambda_4^{kl} C_{64} + \lambda_5^{kl} C_{64} + \lambda_6^{kl} C_{63}\right]
\end{aligned}
\tag{34a}
$$

After substituting expressions for elastic coefficients one obtains:

$$
\begin{aligned}
&b_{11}^{11} = E_1^{(1)} \\
&b_{11}^{22} = b_{11}^{33} = b_{11}^{23} = b_{11}^{13} = b_{11}^{12} = 0,\ b_{22}^{kl} = b_{33}^{kl} = b_{23}^{kl} = b_{13}^{kl} = b_{12}^{kl} = 0
\end{aligned}
\tag{34b}
$$

Here, $E_1^{(1)}$ is the principal Young's modulus of the reinforcement oriented in the y_1 direction. Repeating the procedure for the reinforcement in the y_2 direction yields $b_{22}^{22} = E_1^{(2)}$ with the remaining coefficients equal to zero, and for the reinforcement in the y_3 direction the only non-zero coefficient is $b_{33}^{33} = E_1^{(3)}$.

We are now ready to calculate the effective elastic coefficients of the cubic grid structures of Fig. 5. We denote the length (within the unit cell) and cross-sectional area of the *i-th* reinforcement in the y_i direction by L_i and A_i respectively (in coordinates y_1, y_2, y_3) and the principal Young's modulus of that reinforcement by $E_1^{(i)}$. Then, for a unit cell of volume V, the corresponding volume fraction γ_i is given by $\gamma_i = A_i L_i / V$. Therefore, the non-vanishing effective elastic coefficients for the composite grid-reinforced structure of Fig. 5 are:

$$
\tilde{C}_{11} = \frac{A_1 L_1}{V} E_1^{(1)};\quad \tilde{C}_{22} = \frac{A_2 L_2}{V} E_1^{(2)};\quad \tilde{C}_{33} = \frac{A_3 L_3}{V} E_1^{(3)}
\tag{35a}
$$

The expressions in Eq. (35a) become,

$$
\tilde{C}_{11} = \gamma_1 E_1^{(1)};\quad \tilde{C}_{22} = \gamma_2 E_1^{(2)};\quad \tilde{C}_{33} = \gamma_3 E_1^{(3)}
\tag{35b}
$$

It is observed that all the off-diagonal terms in the effective stiffness matrix are zero. This is partly because the reinforcements in a particular direction have no effect on the stiffness of the structure in the directions perpendicular to it and partly due to the fact that the matrix stiffness is neglected in this model.

4.2 Example 2 - 2D Grid-Reinforced Composite

The second example is used to verify the validity of our model for the case of 2D grid-reinforced structures whereby the reinforcements lie entirely in the $y_1 - y_2$ plane. The pertinent unit cell is shown in Fig. 6. Following the same methodology as in the previous example we first solve for the λ_i^{kl} coefficients from Eq. (31). The resulting expressions are too lengthy to be reproduced here, but once calculated, these coefficients permit the determination of the b_{ij}^{kl} functions as follows:

$$
\begin{aligned}
b_{11}^{11} &= C_{1111} + \lambda_1^{11} C_{11} q_{21} + \lambda_3^{11} C_{22} q_{22} + \lambda_6^{11} C_{13} q_{33} \\
b_{11}^{22} &= C_{1122} + \lambda_1^{22} C_{11} q_{21} + \lambda_3^{22} C_{22} q_{22} + \lambda_6^{22} C_{13} q_{33} \\
b_{11}^{12} &= C_{1112} + \lambda_1^{12} C_{11} q_{21} + \lambda_3^{12} C_{22} q_{22} + \lambda_6^{12} C_{13} q_{33} \\
b_{22}^{11} &= C_{2211} + \lambda_1^{11} C_{21} q_{21} + \lambda_3^{11} C_{22} q_{22} + \lambda_6^{11} C_{23} q_{33} \\
b_{22}^{22} &= C_{2222} + \lambda_1^{22} C_{21} q_{21} + \lambda_3^{22} C_{22} q_{22} + \lambda_6^{22} C_{23} q_{33} \\
b_{22}^{12} &= C_{2212} + \lambda_1^{12} C_{21} q_{21} + \lambda_3^{12} C_{22} q_{22} + \lambda_6^{12} C_{23} q_{33} \\
b_{12}^{11} &= C_{1211} + \lambda_1^{11} C_{66} q_{22} + \lambda_3^{11} C_{66} q_{21} \\
b_{12}^{22} &= C_{1222} + \lambda_1^{22} C_{66} q_{22} + \lambda_3^{22} C_{66} q_{21} \\
b_{12}^{12} &= C_{1212} + \lambda_1^{12} C_{66} q_{22} + \lambda_3^{12} C_{66} q_{21}
\end{aligned}
\tag{36}
$$

The effective elastic coefficients can then be readily determined from Eq. 33(b). We note that the above expressions are valid for generally orthotropic reinforcements. A further simplification can be carried out on these expressions to validate the convergence of our model in the case isotropic reinforcements. In this case, the non-zero local functions b_{ij}^{kl} are

$$b_{11}^{11} = E\cos^4\theta,\ b_{11}^{12} = E\cos^3\theta\sin\theta,\ b_{11}^{22} = b_{12}^{12} = E\cos^2\theta\sin^2\theta \tag{37a}$$

$$b_{22}^{12} = E\cos\theta\sin^3\theta,\ b_{22}^{22} = E\sin^4\theta,\ b_{ij}^{kl} = b_{kl}^{ij} \tag{37b}$$

and the effective coefficients of the structure are:

$$\tilde{C}_{11} = \frac{AL}{V}E\cos^4\theta;\ \ \tilde{C}_{22} = \frac{AL}{V}E\sin^4\theta;\ \ \tilde{C}_{12} = \tilde{C}_{66} = \frac{AL}{V}E\cos^2\theta\,\sin^2\theta \tag{38a}$$

$$\tilde{C}_{16} = \frac{AL}{V}E\cos^3\theta\,\sin\theta;\ \ \tilde{C}_{26} = \frac{AL}{V}E\cos\theta\,\sin^3\theta;\ \ \tilde{C}_{ij} = \tilde{C}_{ji} \tag{38b}$$

These results are the similar to those obtained earlier by Kalamkarov (1992) [41], who used asymptotic homogenization techniques, and by Pshenichnov (1982) [57], who used a different approach based on stress-strain relationships in the reinforcements.

4.3 Example 3 – 3D Grid-Reinforced Composite with Conical Arrangement of Generally Orthotropic Reinforcements

This example pertains to a composite grid structure with a conical arrangement of generally orthotropic reinforcements. The unit cell of this structure (to be referred to in the sequel as S_1) is made of three reinforcements oriented as shown in Fig. 7. The expressions for the effective elastic coefficients are obtained from Eqs. (28), (31), and (33b). Although these expressions are too lengthy to be reproduced here, some of these coefficients will be plotted vs. reinforcement volume fraction or vs. the inclination of the reinforcements with the y_3 axis in the next Section.

4.4 Example 4 - 3D Grid-Reinforced Composite with diagonally Oriented Generally Orthotropic Reinforcements

The composite material structure of this example will be referred to as (S_2). The general unit cell of S_2 is formed by orienting three reinforcements as shown in Fig. 8. Two of the three reinforcements are extended diagonally across the unit cell between two

diametrically opposed vertices while the third reinforcement is spun between the middle of the bottom edge and the middle of the top edge on the opposite face.

The effective elastic coefficients for this structure can be calculated following the same approach used in the previous examples. Although the resulting expressions are too lengthy to be reproduced here, some of the effective coefficients will be represented graphically vs. the relative height of the unit cell in the following Section.

5. Numerical Results and Discussion

The mathematical model and methodology presented in above Sections can be used in analysis and design to tailor the effective elastic coefficients of any three-dimensional composite grid structure by changing the material, number, orientation and/or cross-sectional area and material selection of the reinforcements. In this Section typical effective elastic coefficients will be computed and plotted. For illustration purposes, we will assume that the reinforcements have material properties given in Table 1.

Table 1: Properties of the Reinforcement Material [56]

Property	**Value**
E_1	173.058 GPa
E_2	33.065 GPa
E_3	5.171 GPa
G_{12}	9.377 GPa
G_{13}	8.274 GPa
G_{23}	3.240 GPa
ν_{12}	0.036
ν_{13}	0.250
ν_{23}	0.171

We start with calculation of effective properties of a 3D grid-reinforced composite material shown in Fig. 5. For the purposes of verification of our analytical asymptotic homogenization results we compare them with the numerical results of a Finite Element

calculation. In this calculation we assumed that all elements of 3D grid are made of the same material with the properties provided in the Table 1, with the total volume fraction of reinforcement equal to 0.02, and that matrix is made of epoxy resin with E_M=3.19 GPa and ν_M=0.35. The results of both, analytical and numerical calculations are provided in the Table 2. The agreement between the two sets of values is quite satisfactory.

Table 2. Effective Properties of the Composite Grid-Reinforced Structure shown in Fig. 5

	Asymptotic Homogenization results	**FEM results**
$\tilde{C}_{11}$	4.323 GPa	4.341 GPa
$\tilde{C}_{22}$	3.390 GPa	3.416 GPa
$\tilde{C}_{33}$	3.203 GPa	3.243 GPa

Now let us consider the grid-reinforced structure S_1, shown in Fig. 7, with the conical arrangement of generally orthotropic reinforcements. The numerical results for the effective elastic coefficients of the structure S_1 vs. the reinforcement volume fraction are plotted in Figs. 9 and 10. As expected, the plots show an increase in the effective elastic coefficients as the overall reinforcement volume fraction increases. One also observes that the value of $\tilde{C}_{33}$ in Fig. 10 is significantly higher than the corresponding $\tilde{C}_{11}$ value for the same volume fraction (see Fig. 9). This is a consequence of the reinforcements being more oriented towards the y_3 than the y_1 axis and also the significant disparity between the longitudinal and the transverse stiffnesses of the reinforcement material.

It would also be of interest to plot the variation of the effective coefficients of structure S_1 vs. the angle of inclination of the reinforcements to the y_3 axis. As this angle increases, the reinforcements are oriented progressively closer to the y_1 and the y_2 axes, and, consequently, further away from the y_3 axis. Thus, one anticipates a corresponding increase in the values of $\tilde{C}_{11}$ and $\tilde{C}_{22}$ and a decrease in the value of $\tilde{C}_{33}$. Indeed, Figs. 11-13 illustrate precisely this point.

We now focus our attention to structure S_2 with diagonally oriented generally orthotropic reinforcements shown in Fig. 8. We will plot some of the effective coefficients vs. the relative height of the unit cell. We define the relative height as the ratio of the height to the length of the unit cell. The width of the unit cell and the cross-sectional area of the reinforcements stay the same. Clearly, increasing the relative height of the unit cell will decrease the volume fraction of the reinforcements and at the same time will decrease the orientation angle between the reinforcements and the y_3 axis. Both of these factors tend to reduce the stiffnesses in the y_1 and y_2 directions. Fig. 14 illustrates this point. The stiffness in y_3 direction however increases. This is because the decrease in the angle of inclination of the reinforcements to the y_3 axis (which increases the value of $\tilde{C}_{33}$) dominates the decrease in the volume fraction (which increases the value of $\tilde{C}_{33}$).

Finally, it would be interesting to compare a typical effective coefficient of structures S_1 and S_2 by varying the total volume fraction of the reinforcements. For structure S_1 we do so by varying the cross-sectional area of the reinforcements and for Structure S_2 we do so by changing the relative height of the unit cell. The results are shown in Fig. 15. The general trends depicted in the plot are logical on account of the different manners in

which the volume fraction is varied. For structure S_1 increase the volume fraction by increasing the cross-sectional area of the reinforcements and hence we anticipate a corresponding increase in the value of $\tilde{C}_{33}$. Pertinent to structure S_2 however, by decreasing the relative height of the unit cell (in order to increase the overall reinforcement volume ratio) we simultaneously increase the angle of inclination of the reinforcements with the y_3 axis. Since the reinforcements are now oriented further away from the y_3 axis the value of $\tilde{C}_{33}$ is expected to decrease. Moreover, this decrease dominates the increase in the stiffness value due to the volume fraction increasing. Hence, the net result is an overall decrease in the value of $\tilde{C}_{33}$ albeit in a non-linear manner. Thus, as shown in Fig. 15, beyond a certain volume fraction, S_1 is stiffer than S_2 under these circumstances. This trend can of course be changed. For example, had we increased the volume fraction of S_2 by simply changing the cross-sectional area of the reinforcements and leaving the relative height of the unit cell the same, then a higher volume fraction would translate into a larger $\tilde{C}_{33}$ value. What is important is to realize that the model allows for complete flexibility in designing a structure with desirable mechanical and geometrical characteristics.

6. Conclusions

The asymptotic homogenization method is used to develop a comprehensive three-dimensional micromechanical model pertaining to globally anisotropic periodic composite structures reinforced with an embedded grid of generally orthotropic reinforcements. The generally orthotropy of the material of reinforcements which is very significant from practical point of view renders the problem much more complex. The

model developed transforms the original boundary-value problem into a simpler one characterized by the effective elastic coefficients. These effective coefficients are shown to depend only on the geometric and material parameters of the unit cell and are free from the inhomogeneity complications that characterize their original material counterparts. As a consequence they can be used to study a wide variety of boundary value problems associated with the composite of a given microstructure.

The developed model is applied to different examples of orthotropic composite structures with cubic, conical and diagonal reinforcement orientations. It is shown in these examples that the model allows for complete flexibility in designing a grid-reinforced composite structure with desirable elastic coefficients to conform to any engineering application by changing certain material and/or geometric parameters. Examples of such parameters include the type, number, cross-sectional characteristics and relative orientations of the reinforcements. The asymptotic homogenization results are verified using FEM. It is also shown that in the limiting particular case of 2D grid-reinforced structure with isotropic reinforcements our results converge to those earlier obtained by Kalamkarov (1992) [41], who used asymptotic homogenization techniques, and by Pshenichnov (1982) [57], who used a different approach based on stress-strain relationships in the reinforcements.

Acknowledgements

This work has been supported by the Natural Sciences and Engineering Research Council (NSERC) of Canada and the Brazilian Conselho Nacional de Desenvolvimento Científico (CNPq).

References

[1] Eshelby JD. The determination of the elastic field of an ellipsoidal inclusion, and elated problems. Pro Roy Soc 1957; A241: 376–96.

[2] Hashin Z. The elastic moduli of heterogeneous materials. J Appl Mech 1962;29:143.

[3] Hill R. Elastic properties of reinforced solids. J Mech Phys Solids 1963;11: 357–72.

[4] Hill R. A self-consistent mechanics of composite materials. J Mech Phys Solids 1965; 13: 213–22.

[5] Hashin Z, Shtrikman S. A variational approach to the theory of elastic behavior of multiphase materials. J Mech Phys Solids 1963a;11:127–40.

[6] Hashin Z, Shtrikman, S. Conductivity of polycrystals, Phys Rev Lett 1963b;130 (1): 129–33.

[7] Hashin Z., Rosen, BW. The elastic moduli of fiber-reinforced materials. J Appl Mech 1964;31: 223–32. .

[8] Milton GW. Bounds on the electromagnetic, elastic, and other properties of two-component composites. Phys Rev Lett 1981;46:542–45.

[9] Milton GW. Bounds on the elastic and transport properties of two-component composites. J Mech Phys Solids 1982;30:177–91.

[10] Drugan WJ, Willis JR. A micromechanics-based nonlocal constitutive equation and estimates of representative volume element size for elastic composites. J Mech Phys Solids 1996;44(4):497–524.

[11] Drugan WJ. Two exact micromechanics-based nonlocal constitutive equations for random linear elastic composite materials. J Mech Phys Solids 2003;51(9):1745–72.

[12] Segurado J, LLorca J. A numerical approximation to the elastic properties of sphere-reinforced composites., J Mech Phys Solids 2002;50(10):2107–21.

[13] Budiansky B. On the elastic moduli of some heterogeneous materials. J Mech Phys Solids 1965;13: 223–27.

[14] Russel WB. On the effective moduli of composite materials: effect of fiber length and geometry at dilute concentrations. Zei ang Math und Physik 1973; 24:581–600.

[15] Mori T, Tanaka K. Average stress in matrix and average energy of materials with misfitting inclusions. Acta Metallurgica et Materialia 1973;21: 571–74.

[16] Odegard GM, Gates TS, Wise KE, Park C, Siochi EJ. Constitutive modeling of nanotube-reinforced polymer composites. Comp Sci Tech 2003; 63(11):1671–87.

[17] Sevostianov I. Kachanov M. Homogenization of a nanoparticle with graded interface. Int J of Frac 2006;139:121–27.

[18] Walpole LJ. On bounds for the overall elastic moduli of inhomogeneous systems. J Mech Phys Solids 1966;14(5):151–62.

[19] Walpole LJ. The overall elastic moduli of composite materials. J Mech Phys Solids 1969;17(4):235–51.

[20] Halpin JC. Stiffness and expansion estimate for oriented short fiber composites. J Comp Mat 1969;3:732–34.

[21] Sendeckyj GP. Composite Materials, vol. 2, Mechanics of Composite Materials 1974;45–83 Academic Press, New York.

[22] Hashin Z. Analysis of composite materials–a survey, J Appl Mech 1983;50:481–505.

[23] Torquato S, Stell G. Microstructure of two-phase random media. J Chem Phys 1985;. 82(2):980–87.

[24] Vinson JR, Sierokowski RL. The behavior of Structures Composed of Composite Materials. Nijhoff, Dordrecht: Kluwer Academic Publishers;1986.

[25] Milton GW, Kohn RV. Variational bounds on the effective moduli of anisotropic composites. J Mech Phys Solids 1988;36:597–629.

[26] Teply JL, Dvorak GJ. Bounds on overall instantaneous properties of elastic-plastic composites, J Mech Phys Solids 1988;36:29-58.

[27] Vieira Carneiro, CA, Savi MA. Modeling and simulation of the delamination in composite materials, J. Strain Analysis for Eng Design 2000;35:479-492.

[28] Christensen R.M. A critical evaluation for a class of micromechanics models, J Mech Phys Solids 1990;38: 379–404.

[29] Vasiliev V.V. Mechanics of Composite Structures. Washington DC:Taylor & Francis; 1993.

[30] Kalamkarov AL., Liu. HQ. A new model for the multiphase fiber–matrix composite materials. Composites Part B: Eng 1998;29:643–53.

[31] Zeman J., Šejnoha M. Numerical Evaluation of effective elastic properties of graphite fiber tow impregnated by polymer matrix, J Mech Phys Solids 2001;49:69–90.

[32] Haj Ali R., Kilic H. Nonlinear constitutive models for pultruded FRP composites, Mechanics of Materials 2002;35(8):791–801.

[33] Luccioni MB. Constitutive Model for Fiber-Reinforced Composite Laminates. J Appl Mech 2006;73(6):901–10.

[34] Bensoussan A., Lions JL., Papanicolaou G. Asymptotic analysis for periodic structures, Amsterdam: North-Holland Publ Comp; 1978.

[35] Sanchez-Palencia E. Non-Homogeneous media and vibration theory. Lecture notes in Physics. Berlin: Springer-Verlag; 1980.

[36] Bakhvalov N, Panasenko G. Homogenization: Averaging processes in periodic media. Netherland: Kluwer Academic.Publisher; 1984.

[37] Duvaut G. Analyse fonctionnelle et méchanique des milieux continues. In: Proceeding of the 14th IUTAM Congress, Delft, The Netherlands. 1976. p. 119–32.

[38] Caillerie D. Thin elastic and periodic plates. Math Appl Sci 1984;6:159–91.

[39] Kohn RV, Vogelius M. A new model for thin plates with rapidly varying thickness, Int J Solids Struct 1984;20:333–50.

[40] Kohn RV, Vogelius M. A new model for thin plates with rapidly varying thickness. II. A convergence proof. Quart J Appl Math 1985;43:1–22.

[41] Kalamkarov AL. Composite and Reinforced Elements of Construction. Chichester, New York: Wiley; 1992.

[42] Kalamkarov AL, Kolpakov AG. A new asymptotic model for a composite piezoelastic plate. Int J Solids Struct 2001;38:6027–44.

[43] Kalamkarov AL, Georgiades AV. Modeling of Smart Composites on Account of Actuation, Thermal Conductivity and Hygroscopic Absorption. Composites part B: Eng 2002a;33:141–52.

[44] Kalamkarov AL, Georgiades A.V. Micromechanical Modeling of Smart Composite Structures. Smart Materials Struct 2002b;11:423–34.

[45] Kalamkarov AL, Georgiades AV. Asymptotic Homogenization Models for Smart Composite Plates with Rapidly varying thickness. Part. I. Theory. Int J Multiscale Comput Eng 2004;2(1):133–48.

[46] Georgiades AV, Kalamkarov AL. Asymptotic Homogenization Models for Smart Composite Plates with Rapidly varying thickness. Part II. Applications.International J Multiscale Comput Eng 2004;2(1):149–72.

[47] Georgiades AV, Challagulla KS, Kalamkarov AL. Modeling of the thermopiezoelastic behavior of prismatic smart composite structures made of orthotropic materials. Composites part B: Eng 2006;37:569–582.

[48] Challagulla KS, Georgiades AV, Kalamkarov AL. Asymptotic homogenization modeling of thin network structures. Composites Structures 2007;(3):432–44.

[49] Andrianov IV, Lesnichaya VA, Manevich LI. Homogenization methods in the statics and dynamics of ribbed shells. Moscow: Nauka; 1985.

[50] Challagulla KS, Georgiades AV, Saha GC, Kalamkarov AL. Micromechanical analysis of grid-reinforced thin composite generally orthotropic shells, Composites part B: Eng 2008;39:627-644.

[51] Guedes JM, Kikuchi N. Preprocessing and postprocessing for materials based on the homogenization method with adaptive finite element methods, Computer Meth Appl Mech Eng 1990;83:143–98.

[52] Andrianov, IV, Danishevs'kyy VV, Kalamkarov AL. Asymptotic justification of the three-phase composite model, *Composite Structures* 2006;77(3):395– 404.

[53] Kalamkarov AL, Georgiades AV, Challagulla KS, Saha GC. Micromechanics of Smart Composite Plates with Periodically Embedded Actuators and Rapidly Varying Thickness. J Thermoplastic Compo Mater 2006;19(3):251–76.

[54] Saha GC, Kalamkarov AL, Georgiades AV. Effective elastic characteristics of honeycomb sandwich composite shells made of generally orthotropic materials. Composites Part A: Appl.Sci Manuf 2007a;38:1533–46.

[55] Saha GC, Kalamkarov AL, Georgiades AV. Micromechanical analysis of effective piezoelastic properties of smart composite sandwich shells made of generally orthotropic materials. Smart Mater Struct 2007b;16: 866–83.

[56] Reddy JN. Mechanics of Laminated Composite Plates. New York: CRC Press; 1997.

[57] Pshenichnov GI. Theory of Thin Elastic Network Plates and Shells. Moscow: Nauka; 1982.

Appendix A

$$A_1 = q_{21}^2 C_{11} + q_{22}^2 C_{66} + q_{23}^2 C_{55} + q_{21}q_{22}C_{16} + q_{21}q_{23}C_{15} + q_{22}q_{21}C_{61} + q_{22}q_{23}C_{65} + q_{23}q_{21}C_{51} + q_{23}q_{22}C_{56}$$

$$A_2 = q_{21}q_{31}C_{11} + q_{22}q_{32}C_{66} + q_{23}q_{33}C_{55} + q_{21}q_{32}C_{16} + q_{21}q_{33}C_{15} + q_{22}q_{31}C_{61} + q_{22}q_{33}C_{65} + q_{23}q_{31}C_{51} + q_{23}q_{32}C_{56}$$

$$A_3 = q_{21}q_{22}C_{12} + q_{21}q_{22}C_{66} + q_{21}^2 C_{16} + q_{21}q_{23}C_{14} + q_{22}^2 C_{62} + q_{22}q_{23}C_{64} + q_{23}q_{21}C_{56} + q_{23}q_{22}C_{52} + q_{23}^2 C_{54}$$

$$A_4 = q_{21}q_{32}C_{12} + q_{22}q_{31}C_{66} + q_{21}q_{31}C_{16} + q_{21}q_{33}C_{14} + q_{22}q_{32}C_{62} + q_{22}q_{33}C_{64} + q_{23}q_{31}C_{56} + q_{23}q_{32}C_{52} + q_{23}q_{33}C_{54}$$

$$A_5 = q_{21}q_{23}C_{13} + q_{21}q_{23}C_{55} + q_{21}^2 C_{15} + q_{21}q_{22}C_{14} + q_{22}q_{21}C_{65} + q_{22}^2 C_{64} + q_{22}q_{23}C_{63} + q_{23}q_{22}C_{54} + q_{23}^2 C_{53}$$

$$A_6 = q_{21}q_{33}C_{13} + q_{23}q_{31}C_{55} + q_{21}q_{31}C_{15} + q_{21}q_{32}C_{14} + q_{22}q_{31}C_{65} + q_{22}q_{32}C_{64} + q_{22}q_{33}C_{63} + q_{23}q_{32}C_{54} + q_{23}q_{33}C_{53}$$

$$A_7 = q_{21}C_{11kl} + q_{22}C_{12kl} + q_{23}C_{13kl}$$

$$A_8 = q_{21}q_{31}C_{11} + q_{22}q_{32}C_{66} + q_{23}q_{33}C_{55} + q_{31}q_{22}C_{16} + q_{31}q_{23}C_{15} + q_{32}q_{21}C_{61} + q_{32}q_{23}C_{65} + q_{33}q_{21}C_{51} + q_{33}q_{22}C_{56}$$

$$A_9 = q_{31}^2 C_{11} + q_{32}^2 C_{66} + q_{33}^2 C_{55} + q_{31}q_{32}C_{16} + q_{31}q_{33}C_{15} + q_{32}q_{31}C_{61} + q_{32}q_{33}C_{65} + q_{33}q_{31}C_{51} + q_{33}q_{32}C_{56}$$

$$A_{10} = q_{31}q_{22}C_{12} + q_{21}q_{32}C_{66} + q_{31}q_{21}C_{61} + q_{31}q_{23}C_{14} + q_{32}q_{22}C_{62} + q_{32}q_{23}C_{64} + q_{33}q_{21}C_{56} + q_{33}q_{22}C_{52} + q_{33}q_{23}C_{54}$$

$$A_{11} = q_{31}q_{32}C_{12} + q_{32}q_{31}C_{66} + q_{31}^2 C_{16} + q_{31}q_{33}C_{14} + q_{32}^2 C_{62} + q_{32}q_{33}C_{64} + q_{33}q_{31}C_{65} + q_{33}q_{32}C_{52} + q_{33}^2 C_{54}$$

$$A_{12} = q_{31}q_{23}C_{13} + q_{21}q_{33}C_{55} + q_{31}q_{21}C_{15} + q_{31}q_{22}C_{14} + q_{32}q_{21}C_{65} + q_{32}q_{22}C_{64} + q_{32}q_{23}C_{63} + q_{33}q_{22}C_{54} + q_{33}q_{23}C_{53}$$

$$A_{13} = q_{31}q_{33}C_{13} + q_{33}q_{31}C_{55} + q_{31}^2 C_{15} + q_{31}q_{32}C_{14} + q_{32}q_{31}C_{65} + q_{32}^2 C_{64} + q_{32}q_{33}C_{63} + q_{33}q_{32}C_{54} + q_{33}^2 C_{53}$$

$$A_{14} = q_{31}C_{11kl} + q_{32}C_{12kl} + q_{33}C_{13kl}$$

$$A_{15} = q_{21}q_{22}C_{66} + q_{21}q_{22}C_{12} + q_{21}^2 C_{61} + q_{21}q_{23}C_{65} + q_{22}^2 C_{62} + q_{22}q_{23}C_{25} + q_{23}q_{21}C_{41} + q_{23}q_{22}C_{46} + q_{23}^2 C_{45}$$

$$A_{16} = q_{21}q_{32}C_{66} + q_{22}q_{31}C_{12} + q_{31}q_{21}C_{61} + q_{21}q_{33}C_{65} + q_{22}q_{32}C_{26} + q_{22}q_{33}C_{25} + q_{23}q_{31}C_{41} + q_{23}q_{32}C_{46} + q_{23}q_{33}C_{45}$$

$$A_{17} = q_{21}^2 C_{66} + q_{22}^2 C_{22} + q_{23}^2 C_{44} + q_{21}q_{22}C_{62} + q_{21}q_{23}C_{64} + q_{22}q_{21}C_{26} + q_{22}q_{23}C_{24} + q_{23}q_{21}C_{46} + q_{23}q_{22}C_{42}$$

$$A_{18} = q_{21}q_{31}C_{66} + q_{22}q_{32}C_{22} + q_{23}q_{33}C_{44} + q_{21}q_{32}C_{62} + q_{21}q_{33}C_{64} + q_{22}q_{31}C_{26} + q_{22}q_{33}C_{24} + q_{23}q_{31}C_{46} + q_{23}q_{32}C_{42}$$

$$A_{19} = q_{22}q_{23}C_{23} + q_{22}q_{23}C_{44} + q_{21}^2 C_{65} + q_{21}q_{22}C_{64} + q_{21}q_{23}C_{63} + q_{22}q_{21}C_{25} + q_{22}^2 C_{24} + q_{23}q_{21}C_{45} + q_{32}^2 C_{43}$$

$$A_{20} = q_{22}q_{33}C_{23} + q_{23}q_{32}C_{44} + q_{21}q_{31}C_{65} + q_{21}q_{32}C_{64} + q_{21}q_{33}C_{63} + q_{22}q_{31}C_{25} + q_{22}q_{32}C_{24} + q_{23}q_{31}C_{45} + q_{23}q_{33}C_{43}$$

$$A_{21} = q_{21}C_{12kl} + q_{22}C_{22kl} + q_{23}C_{23kl}$$

$$A_{22} = q_{31}q_{22}C_{66} + q_{21}q_{32}C_{21} + q_{31}q_{21}C_{61} + q_{31}q_{23}C_{65} + q_{32}q_{22}C_{62} + q_{32}q_{23}C_{25} + q_{33}q_{21}C_{41} + q_{33}q_{22}C_{46} + q_{33}q_{23}C_{45}$$

$$A_{23} = q_{31}q_{32}C_{66} + q_{32}q_{31}C_{21} + q_{31}^2 C_{61} + q_{31}q_{33}C_{65} + q_{32}^2 C_{26} + q_{32}q_{33}C_{25} + q_{33}q_{31}C_{41} + q_{33}q_{32}C_{46} + q_{33}^2 C_{45}$$

$$A_{24} = q_{21}q_{31}C_{66} + q_{22}q_{32}C_{22} + q_{23}q_{33}C_{44} + q_{31}q_{22}C_{62} + q_{31}q_{23}C_{64} + q_{32}q_{21}C_{26} + q_{32}q_{23}C_{24} + q_{33}q_{21}C_{46} + q_{33}q_{22}C_{42}$$

$$A_{25} = q_{31}^2 C_{66} + q_{32}^2 C_{22} + q_{33}^2 C_{44} + q_{31}q_{32}C_{62} + q_{31}q_{33}C_{64} + q_{32}q_{31}C_{26} + q_{32}q_{33}C_{24} + q_{33}q_{31}C_{46} + q_{33}q_{32}C_{42}$$

$$A_{26} = q_{32}q_{23}C_{23} + q_{22}q_{33}C_{44} + q_{31}q_{21}C_{65} + q_{31}q_{22}C_{64} + q_{31}q_{23}C_{63} + q_{32}q_{21}C_{25} + q_{32}q_{22}C_{24} + q_{33}q_{21}C_{45} + q_{33}q_{23}C_{43}$$

$$A_{27} = q_{32}q_{33}C_{23} + q_{33}q_{32}C_{44} + q_{31}^2 C_{65} + q_{31}q_{32}C_{64} + q_{31}q_{33}C_{63} + q_{32}q_{31}C_{25} + q_{32}^2 C_{24} + q_{33}q_{31}C_{45} + q_{33}^2 C_{43}$$

$$A_{28} = q_{31}C_{12kl} + q_{32}C_{22kl} + q_{33}C_{23kl}$$

$$A_{29} = q_{21}q_{23}C_{55} + q_{21}q_{23}C_{13} + q_{21}^2 C_{51} + q_{21}q_{22}C_{56} + q_{22}q_{21}C_{41} + q_{22}^2 C_{46} + q_{22}q_{23}C_{45} + q_{23}q_{22}C_{36} + q_{23}^2 C_{35}$$

$$A_{30} = q_{21}q_{33}C_{55} + q_{23}q_{31}C_{13} + q_{21}q_{31}C_{51} + q_{21}q_{32}C_{56} + q_{22}q_{31}C_{41} + q_{22}q_{32}C_{46} + q_{22}q_{33}C_{45} + q_{23}q_{32}C_{36} + q_{23}q_{33}C_{35}$$

$$A_{31} = q_{22}q_{23}C_{44} + q_{22}q_{23}C_{23} + q_{21}^2C_{56} + q_{21}q_{22}C_{52} + q_{21}q_{23}C_{54} + q_{22}q_{21}C_{46} + q_{22}^2C_{42} + q_{23}q_{21}C_{36} + q_{23}^2C_{34}$$

$$A_{32} = q_{22}q_{33}C_{44} + q_{23}q_{32}C_{23} + q_{21}q_{31}C_{56} + q_{21}q_{32}C_{52} + q_{21}q_{33}C_{54} + q_{22}q_{31}C_{46} + q_{22}q_{32}C_{42} + q_{23}q_{31}C_{36} + q_{23}q_{33}C_{34}$$

$$A_{33} = q_{21}{}^2C_{55} + q_{22}{}^2C_{44} + q_{23}{}^2C_{33} + q_{21}q_{22}C_{54} + q_{21}q_{23}C_{53} + q_{22}q_{21}C_{45} + q_{22}q_{23}C_{43} + q_{23}q_{21}C_{35} + q_{23}q_{22}C_{34}$$

$$A_{34} = q_{21}q_{31}C_{55} + q_{22}q_{32}C_{44} + q_{23}q_{33}C_{33} + q_{21}q_{32}C_{54} + q_{21}q_{33}C_{53} + q_{22}q_{31}C_{45} + q_{22}q_{33}C_{43} + q_{23}q_{31}C_{35} + q_{23}q_{32}C_{34}$$

$$A_{35} = q_{21}C_{13kl} + q_{22}C_{23kl} + q_{23}C_{33kl}$$

$$A_{36} = q_{31}q_{23}C_{55} + q_{21}q_{33}C_{13} + q_{31}q_{21}C_{51} + q_{31}q_{22}C_{56} + q_{32}q_{21}C_{41} + q_{32}q_{22}C_{46} + q_{32}q_{23}C_{45} + q_{33}q_{22}C_{36} + q_{33}q_{23}C_{35}$$

$$A_{37} = q_{31}q_{33}C_{55} + q_{33}q_{31}C_{13} + q_{31}^2C_{51} + q_{31}q_{32}C_{56} + q_{32}q_{31}C_{41} + q_{32}^2C_{46} + q_{32}q_{33}C_{45} + q_{33}q_{32}C_{36} + q_{33}^2C_{35}$$

$$A_{38} = q_{23}q_{32}C_{44} + q_{33}q_{22}C_{23} + q_{31}q_{21}C_{56} + q_{31}q_{22}C_{52} + q_{31}q_{23}C_{54} + q_{32}q_{21}C_{46} + q_{32}q_{22}C_{42} + q_{33}q_{21}C_{36} + q_{33}q_{23}C_{34}$$

$$A_{39} = q_{32}q_{33}C_{44} + q_{33}q_{32}C_{23} + q_{31}^2C_{56} + q_{31}q_{32}C_{52} + q_{31}q_{33}C_{54} + q_{32}q_{31}C_{46} + q_{32}^2C_{42} + q_{33}q_{31}C_{36} + q_{33}^2C_{34}$$

$$A_{40} = q_{21}q_{31}C_{55} + q_{22}q_{32}C_{44} + q_{23}q_{33}C_{33} + q_{31}q_{22}C_{54} + q_{31}q_{23}C_{53} + q_{32}q_{21}C_{45} + q_{32}q_{23}C_{43} + q_{33}q_{21}C_{35} + q_{33}q_{22}C_{34}$$

$$A_{41} = q_{31}{}^2C_{55} + q_{32}{}^2C_{44} + q_{33}{}^2C_{33} + q_{31}q_{32}C_{54} + q_{31}q_{33}C_{53} + q_{32}q_{31}C_{45} + q_{32}q_{33}C_{43} + q_{33}q_{31}C_{35} + q_{33}q_{32}C_{34}$$

$$A_{42} = q_{31}C_{13kl} + q_{32}C_{23kl} + q_{33}C_{33kl}$$

Table 1: Properties of the Reinforcement Material [56]

Property	**Value**
E_1	173.058 GPa
E_2	33.065 GPa
E_3	5.171 GPa
G_{12}	9.377 GPa
G_{13}	8.274 GPa
G_{23}	3.240 GPa
ν_{12}	0.036
ν_{13}	0.250
ν_{23}	0.171

Table 2. Effective Properties of the Composite Grid-Reinforced Structure shown in Fig. 5

	Asymptotic Homogenization results	**FEM results**
$\tilde{C}_{11}$	4.323 GPa	4.341 GPa
$\tilde{C}_{22}$	3.390 GPa	3.416 GPa
$\tilde{C}_{33}$	3.203 GPa	3.243 GPa

List of Figure Captions

Fig. 14. Plot of $\tilde{C}_{11}$, $\tilde{C}_{22}$, $\tilde{C}_{33}$, and $\tilde{C}_{66}$ effective coefficient vs. relative height of the unit cell for structure S_2 shown in Fig. 8.

Fig. 15. Plot of $\tilde{C}_{33}$ vs. total volume fraction for structures S_1 (7) and S_2 (8).

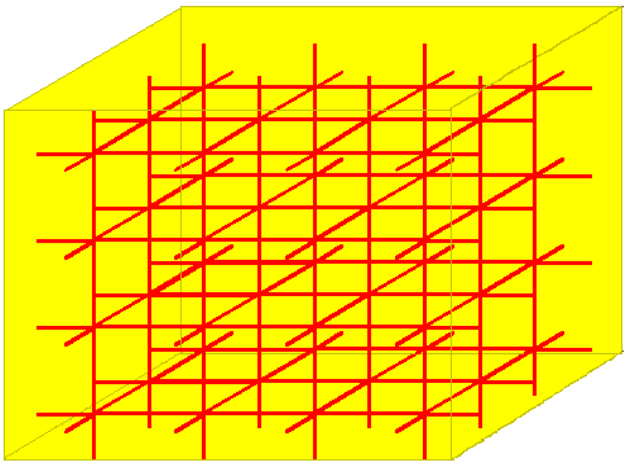

Fig. 1. Three-Dimensional Grid Reinforced Composite Structure.

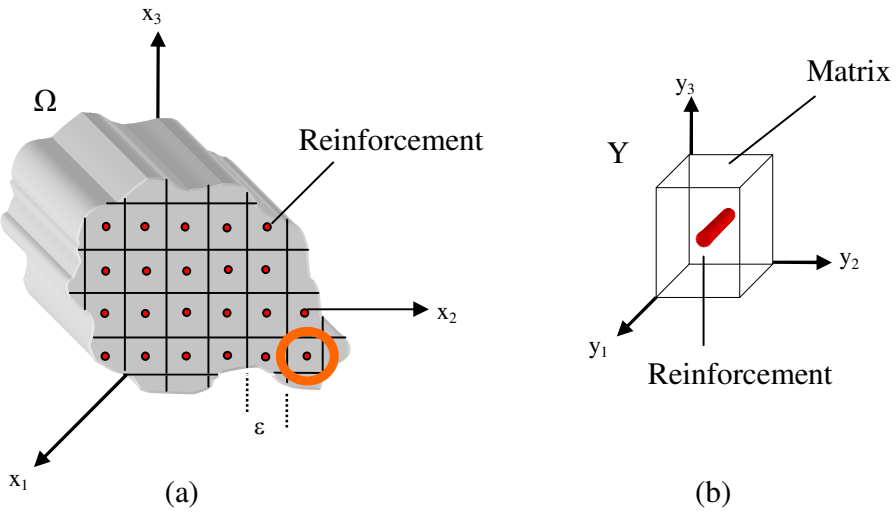

Fig. 2. (a) Three-Dimensional composite structure, (b) representative unit cell Y.

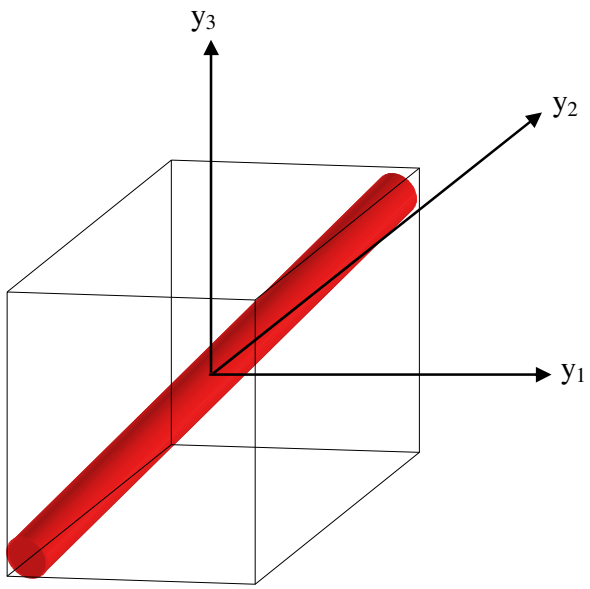

Fig. 3. Unit cell of grid reinforced composite with a single reinforcement family.

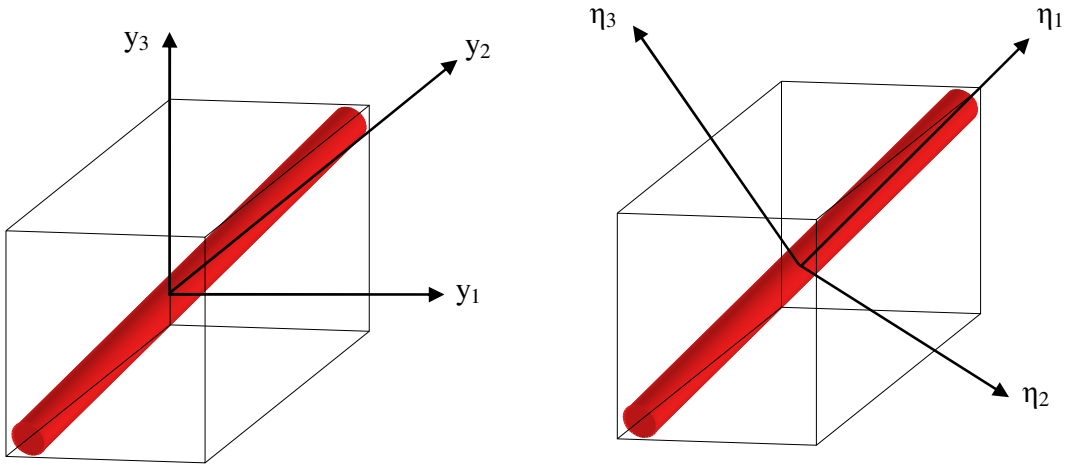

Fig. 4. Unit cell in original and rotated microscopic coordinates.

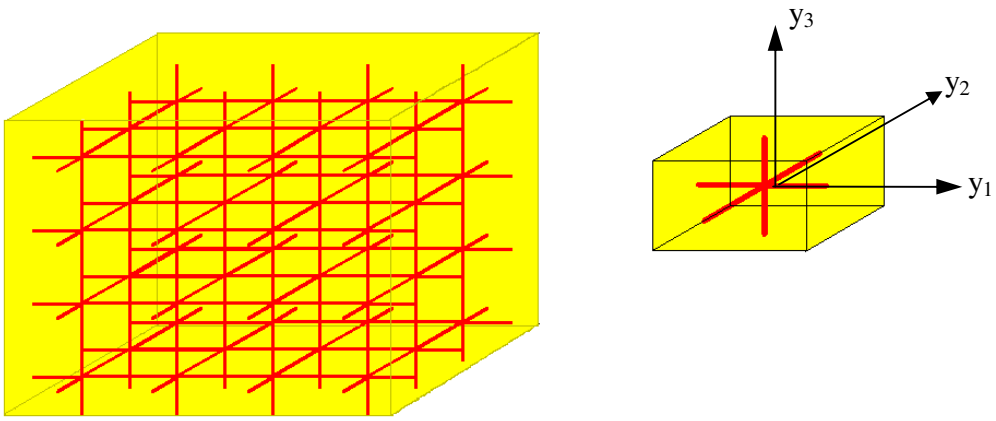

Fig. 5. Unit cell of the cubic grid-reinforced structure with reinforcements in y_1, y_2, y_3 directions.

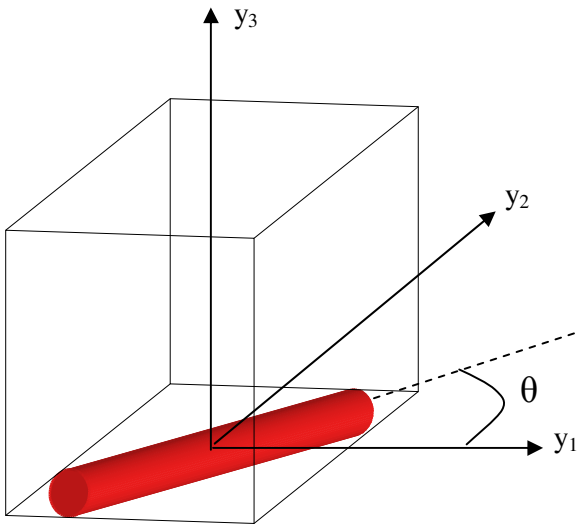

Fig. 6. Unit cell for 2D structure with reinforcements in the $y_1 - y_2$ plane.

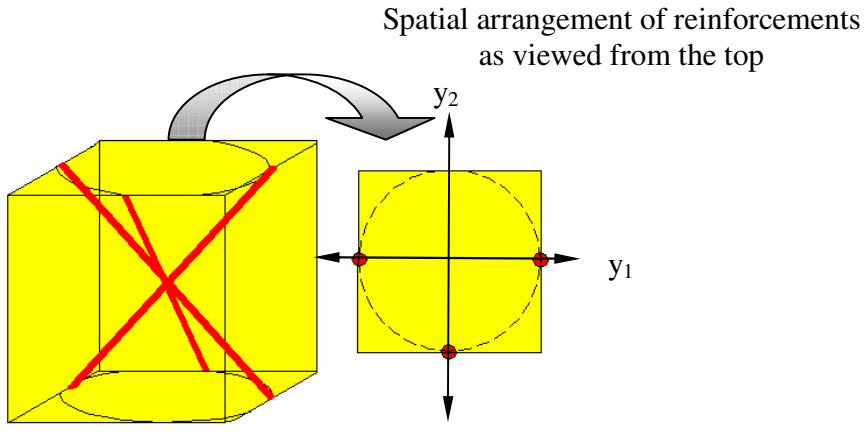

Fig. 7. Unit cell for composite grid structure with conical arrangement of generally orthotropic reinforcements (Structure S_1)

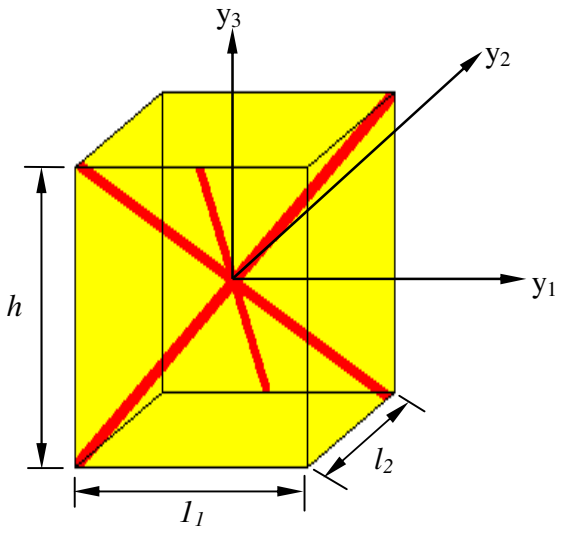

Fig. 8. Unit cell for composite grid structure with diagonally oriented generally orthotropic reinforcements (Structure S_2).

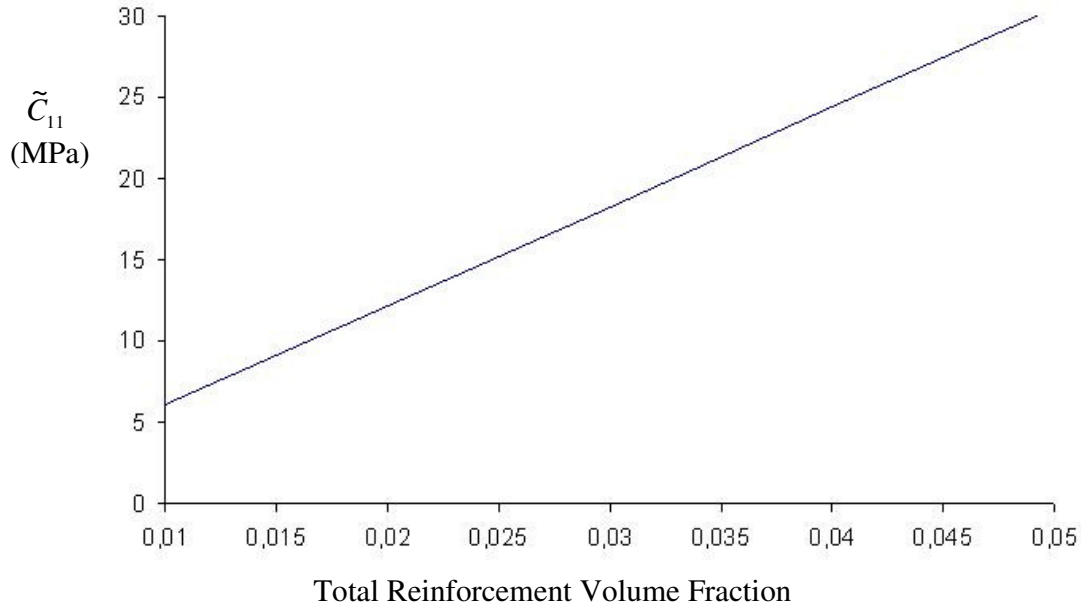

Fig. 9. Plot of $\tilde{C}_{11}$ vs. reinforcement volume fraction for structure S_1.

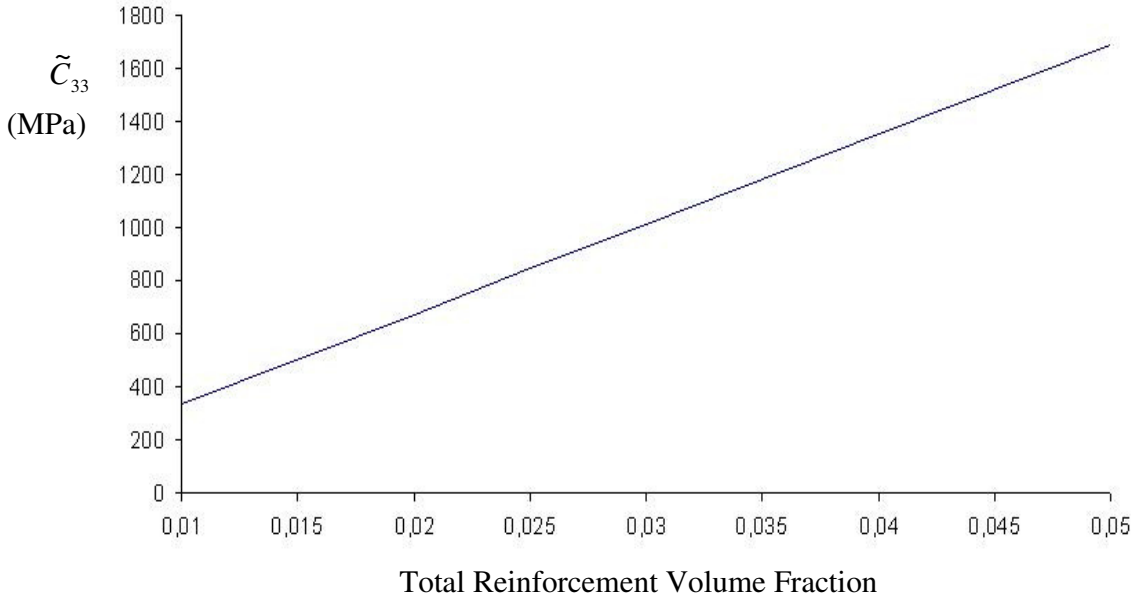

Fig. 10. Plot of $\tilde{C}_{33}$ vs. reinforcement volume fraction for structure S_1.

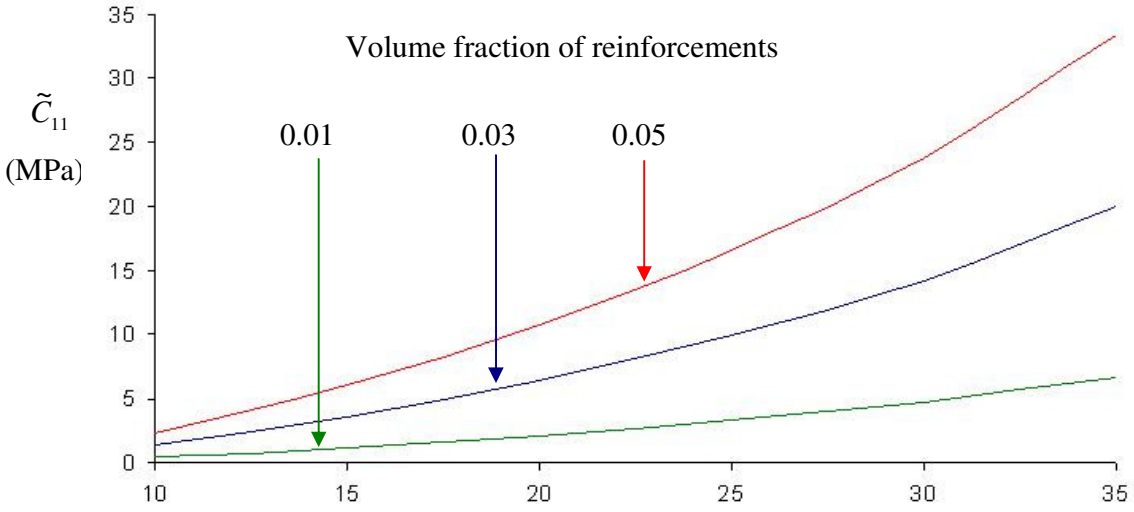

Fig. 11. Plot of the $\tilde{C}_{11}$ effective elastic coefficient vs. inclination of reinforcements with the y_3 axis pertaining to structure S_1 for reinforcement volume fractions equal to 0.01, 0.03, and 0.05.

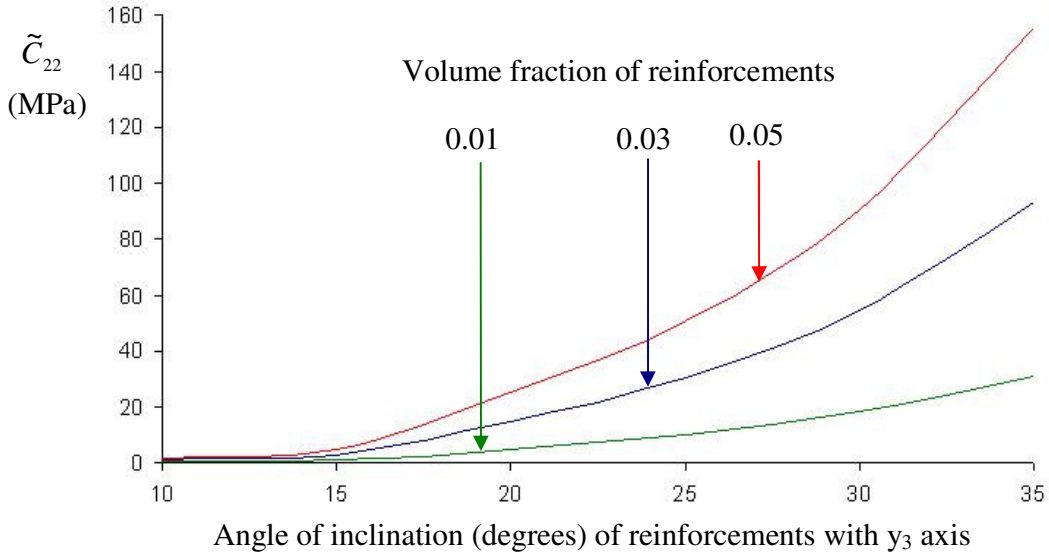

Fig. 12. Plot of the $\tilde{C}_{22}$ effective elastic coefficient vs. inclination of reinforcements with the y_3 axis pertaining to structure S_1 for reinforcement volume fractions equal to 0.01, 0.03, and 0.05.

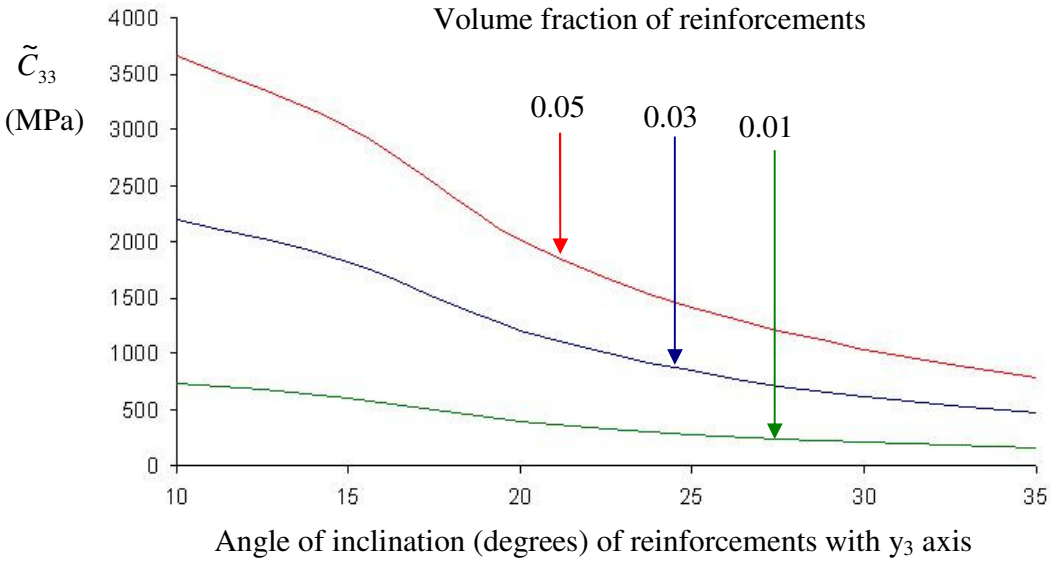

Fig. 13. Plot of the $\tilde{C}_{33}$ effective elastic coefficient vs. inclination of reinforcements with the y_3 axis pertaining to structure S_1 for reinforcement volume fractions equal to 0.01, 0.03, and 0.05.

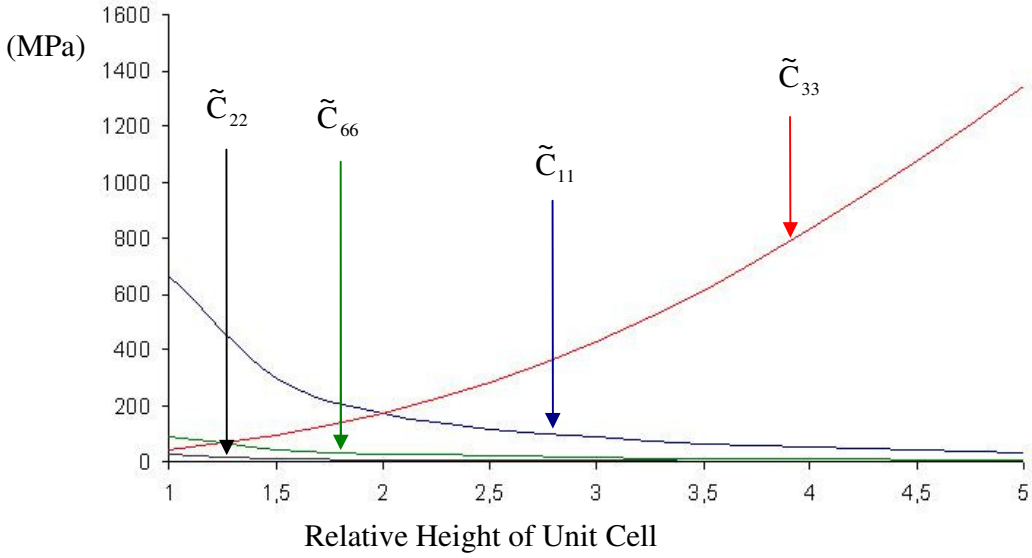

Fig. 14. Plot of $\tilde{C}_{11}$, $\tilde{C}_{22}$, $\tilde{C}_{33}$, and $\tilde{C}_{66}$ effective coefficient vs. relative height of the unit cell for structure S_2 shown in Fig. 8.

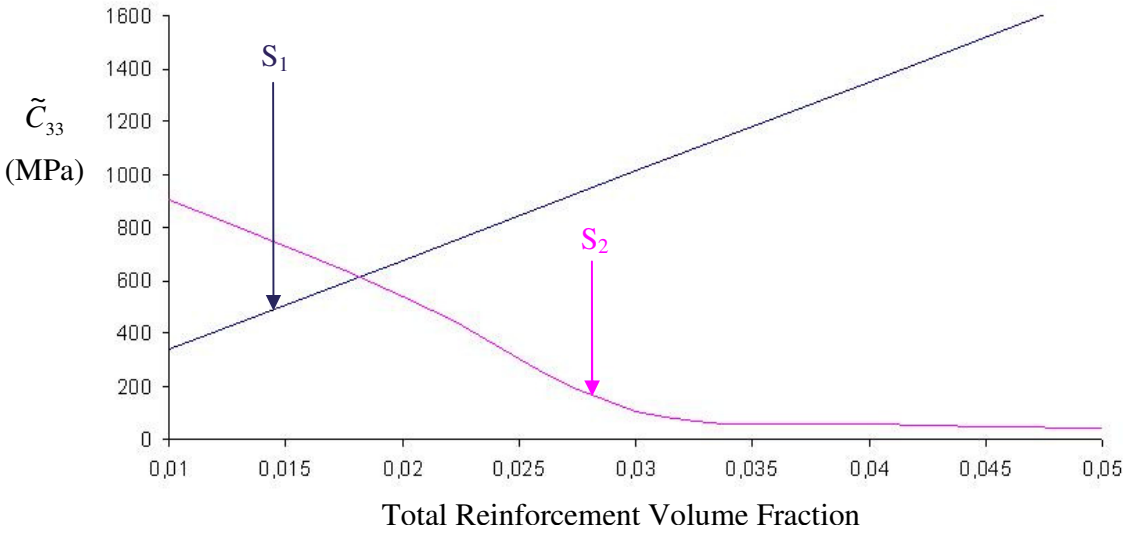

Fig. 15. Plot of $\tilde{C}_{33}$ vs. total volume fraction for structures S_1 (Fig. 7) and S_2 (Fig. 8).